

# Modified AASHTO empirical pavement design method for geosynthetic-reinforced asphalt

G. H. Roodi<sup>1</sup>, V. V. Kumar<sup>2</sup>, S. Subramanian<sup>3</sup> and J. G. Zornberg<sup>4</sup>

<sup>1</sup>HDR Inc., Toronto, Canada, E-mail: gholamhossein.roodi@hdrinc.com (corresponding author)

<sup>2</sup>Huesker Inc., Leander, TX, USA, E-mail: vkumar@huesker.com

<sup>3</sup>The Transtec Group Inc., Austin, TX, USA, E-mail: subu@thetranstecgroup.com

<sup>4</sup>Department of Civil, Architectural and Environmental Engineering, University of Texas at Austin, Austin, TX, USA, E-mail: zornberg@mail.utexas.edu

Received 16 April 2025, accepted 09 July 2025

**ABSTRACT:** Geosynthetics are commonly adopted to retard problems associated with reflective cracking in asphalt, although their inclusion as asphalt reinforcements also provides structural benefits. However, methodologies are yet to develop to incorporate these structural benefits into design. This study proposes a design method to account for structural capacity increase by geosynthetics in asphalt. The proposed method relies on quantifying a tensile strain reduction ratio ( $\alpha$ ) defined as the ratio between elastic tensile strain in HMA in a geosynthetic-reinforced asphalt road and that in an equivalent unreinforced road. Implementation of the design method involves incorporating a modified structural number or modified ESAL into AASHTO1993 design by using an equivalent modulus or an equivalent axle load factor for asphalt-geosynthetic composite. The geosynthetic benefits were ultimately accounted for in design either by reducing the asphalt thickness or by increasing the traffic volume. This paper presents the results of parametric evaluations of geosynthetic benefits for  $\alpha$  ranging from 0.8 to 0.4. Design charts were developed to facilitate adoption of the proposed design method, and a design example is provided to illustrate the predicted benefits. It was found that 20% to 33% reduction in asphalt thickness, or 1.8- to 4.0-fold increase in traffic volume, is feasible.

**KEYWORDS:** Geosynthetics, Reinforcements, Reinforced Pavement Design, Asphalt Thickness Reduction, Traffic Benefit Ratio, Interlayer, Fatigue Crack, Increased Traffic Volume

**REFERENCE:** Roodi, G. H., Kumar, V. V., Subramanian, S. and Zornberg, J. G. (2026). Modified AASHTO empirical pavement design method for geosynthetic-reinforced asphalt. *Geosynthetics International*, 33, No. 2, 326–344. [<https://doi.org/10.1680/jgein.25.00056>]

## 1. INTRODUCTION

Although a common objective for using geosynthetic interlayers in hot mix asphalt (HMA) is to retard or eliminate problems associated with reflective cracking in structural asphalt overlays, it has become clear that their inclusion as asphalt reinforcements provides additional structural benefits to the pavement system. Despite a wide range of documented benefits from geosynthetic reinforcement of an asphalt layer, limited methodologies have been developed to incorporate such benefits into pavement design. Design methodologies for geosynthetic-reinforced unpaved roadways (e.g. Stewart *et al.* 1977; Giroud and Noiray 1981; Giroud and Han 2004) and roadways with geosynthetic-stabilized base layers (e.g. Berg *et al.* 2000) are comparatively more established.

Design methodologies that have been developed for the roadways with geosynthetic-stabilized unbound aggregate layers typically express design benefits in terms of reduction in the unbound aggregate layer thickness (often referred to as reduced base thickness) or extended traffic volume. They typically define the experimentally measured Traffic Benefit Ratio (TBR) and Base Course Reduction (BCR) to quantify benefits from using geosynthetics in the base layer (e.g. Berg *et al.* 2000; AASHTO 2009). The TBR is defined as the ratio between the traffic volume on a geosynthetic-stabilized roadway and that on an equivalent unreinforced roadway for a prescribed rut depth. The BCR is defined as the percent reduction in base course thickness due to the inclusion of a geosynthetic product in the base layer. Such benefits have often been observed in performance differences between full-scale or experimental sections

constructed with and without geosynthetics (e.g. Al-Qadi *et al.* 2006; Cuelho *et al.* 2014; Tang *et al.* 2014; Sprague and Sprague 2016). Additional design methodologies have also been developed by formulating mechanistic-empirical procedures to quantify the benefits from adopting geosynthetics for base stabilization (e.g. Perkins *et al.* 2004).

In comparison, design methodologies for geosynthetic-reinforced asphalt roadways have been comparatively more limited. Among others, methodologies based on French design philosophies and South African design methods are notable. Freire *et al.* (2023) have proposed a two-step design procedure for geosynthetic-reinforced asphalt based on the French design philosophy. In the Freire *et al.* method, the number of admissible equivalent axle loads, as defined by the standard French pavement design method, is separately calculated for the two steps, then added together to obtain the total number of admissible equivalent axle loads for the geosynthetic-reinforced asphalt road. In the first step, the contribution of geosynthetic reinforcement is ignored and pavement is designed according to the standard French pavement design method. In the second step, Freire *et al.* (2023) assume that the asphalt layers below the geosynthetic reinforcement are disintegrated and the layers above the geosynthetic are damaged. In this step, the contribution of geosynthetic reinforcement is considered by using two constants (one for fatigue in the asphalt layer and one for rutting in the granular layer) to calculate the additional number of admissible equivalent axle loads.

South African Bitumen Association Technical Guidelines on Asphalt Reinforcement for Road Construction (SABITA TG3 2022) has detailed two methodologies for the design of geosynthetic-reinforced asphalt based on Paris's fracture law for initiation and propagation of cracks in asphalt (Lytton 1989). The Molenaar method (Molenaar 1995; Molenaar and Nods 1996) uses predetermined stress-intensity factors for bending, shear, and thermal modes of cracking as a function of crack length ratio. In this method, asphalt fracture properties are determined either from published databases or from three-point bending beam fatigue tests. The Molenaar method incorporates the impact of geosynthetic reinforcement into the pavement design by adopting fracture ratio, which is the ratio between fracture energies in bending beam fatigue tests of asphalt samples with and without geosynthetic reinforcement (Kunst and Kirschner 1993). This design method determines either the geosynthetic-reinforced asphalt thickness (for a given traffic volume) or the traffic volume (for a given asphalt thickness).

The second design method adopted by the South African technical guidelines has been developed by Brown *et al.* (1999, 2001) and is formulated into two software programs: OLCRACK (for asphalt overlay design for traffic loads) and THERMCR (for asphalt overlay design for thermal loads). The Brown *et al.* method proposes a strain-based iterative modification procedure to incorporate the impact of geosynthetic reinforcement into the pavement design. In this method,

asphalt fracture properties are determined using the indirect tensile fatigue test. The asphalt fracture properties along with other mechanical and geometrical properties of asphalt, geosynthetic, and asphalt-geosynthetic interface are then used as input parameters into a mechanistic model to produce crack development predictions. Ultimately, the Brown *et al.* method predicts the traffic volume (for a given asphalt thickness).

The previous research endeavors on geosynthetic benefits in asphalt layers have mainly focused on benefits other than increased structural capacity, with a particular focus on the use of geosynthetic to mitigate reflective cracking (e.g. Elseifi 2003; Ferrotti *et al.* 2012; Lytton 1989; Pasquini *et al.* 2014; Roodi *et al.* 2023; Saride and Kumar 2017; Solatiyan *et al.* 2020; Zornberg 2017). However, other investigations suggest that the geosynthetic reinforcement of asphalt may also result in an increased structural capacity (e.g. Correia and Zornberg 2016; Graziani *et al.* 2014; Kumar *et al.* 2021a 2021b; Zofka and Maliszewski 2019). Specifically, in recent full-scale field studies by Kumar *et al.* (2022, 2025) a series of controlled traffic loadings were conducted on sensor-instrumented unreinforced and geosynthetic-reinforced asphalt roadway sections to quantify and subsequently compare their structural capacity. The controlled traffic loadings involved driving 80-kN (18-kips) standard single axle as well as light axle loads directly above sensors (asphalt strain gauges) that had been installed at the bottom of the asphalt layer. Significantly smaller tensile strains in the geosynthetic-reinforced sections were recorded compared to those recorded in the unreinforced section under both standard axle and light axle loads. Accordingly, Kumar *et al.* (2022, 2025) introduced a tensile strain reduction ratio ( $\alpha$ ), which is defined as the ratio between the elastic tensile strain at the bottom of the Hot Mix Asphalt (HMA) layer in a geosynthetic-reinforced asphalt road and that in an equivalent unreinforced road.

In this study, a modification to the AASHTO (1993) empirical design method is proposed for flexible pavements with geosynthetic-reinforced asphalt. The design method relies on the availability of the tensile strain reduction ratio ( $\alpha$ ) measured under the 80-kN (18-kips) standard single axle load. Based on a comprehensive field evaluation, Kumar *et al.* (2022, 2025) determined that the  $\alpha$  value for a wide range of geosynthetic reinforcements and pavement conditions may range from 1.0 (insignificant enhancement by geosynthetic reinforcement) to 0.1 (significantly enhanced performance by geosynthetic reinforcement).

The proposed modified design approach incorporates a modified structural number (SN) or a modified Equivalent Single Axle Load (ESAL) to the AASHTO (1993) empirical pavement design procedure, by adopting two approaches including the use of an equivalent (increased) modulus (Approach 1) or an equivalent axle load factor for asphalt-geosynthetic composite (Approach 2). While each approach uses a different concept to account for the benefits from using geosynthetic reinforcements within the HMA layer, they both are

formulated to achieve the same design objectives of reducing the asphalt thickness (for a given traffic volume) or increasing the traffic volume (for a given asphalt thickness).

## 2. MODIFIED AASHTO EMPIRICAL PAVEMENT DESIGN METHOD FOR HMA-GS COMPOSITE

A common approach to evaluate benefits of adopting geosynthetics in roadways is to compare the performances of identical roadway sections that were constructed with and without geosynthetics. The traffic benefit ratio (TBR) for geosynthetic-stabilized unbound aggregate layer, for example, determines the ratio between traffic volumes in full or reduced scale sections with and without geosynthetic at the same rut depth. Similarly, the modified AASHTO empirical design method for HMA-GS Composite proposed in this study relies on the availability of performance data from full-scale roadways constructed with and without geosynthetic reinforcement in their asphalt layer. As illustrated in Figure 1, as part of a comprehensive field experiment, Kumar *et al.* (2022, 2025) constructed several instrumented highway sections to quantify the structural benefits expected from geosynthetic reinforcements placed in the asphalt layer. Geosynthetic-reinforced asphalt road sections were constructed alongside and side-by-side of

equivalent unreinforced road sections and loaded by controlled traffic of the 80-kN (18-kips) standard single axle load. The elastic tensile strain at the bottom of the asphalt layer was measured in each section using asphalt strain gauges (ASG). The ratio between the elastic tensile strain at the bottom of the HMA layer in a geosynthetic-reinforced asphalt road and that in an equivalent unreinforced road was defined as tensile strain reduction ratio ( $\alpha$ ):

$$\alpha = \frac{\varepsilon_{HGC}}{\varepsilon_{HMA}} \quad (1)$$

where  $\varepsilon_{HGC}$  and  $\varepsilon_{HMA}$  are the elastic tensile strains at the bottom of the HMA layer in geosynthetic-reinforced asphalt and unreinforced roads, respectively.

The proposed modified AASHTO empirical design method for HMA-GS Composite uses  $\alpha$  to provide modifications to the AASHTO (1993) empirical unreinforced pavement design procedure so that it can be applied to geosynthetic-reinforced asphalt roads. Two approaches are presented in this paper to implement the proposed design method. The first approach involves determining an equivalent (increased) modulus of HMA-GS Composite ( $E_{HGC}$ ), which is subsequently used to obtain an equivalent (increased) layer coefficient for the HMA layer. The equivalent (increased) layer coefficient is then used to determine an equivalent (increased) SN, and thus, an increased traffic volume, or

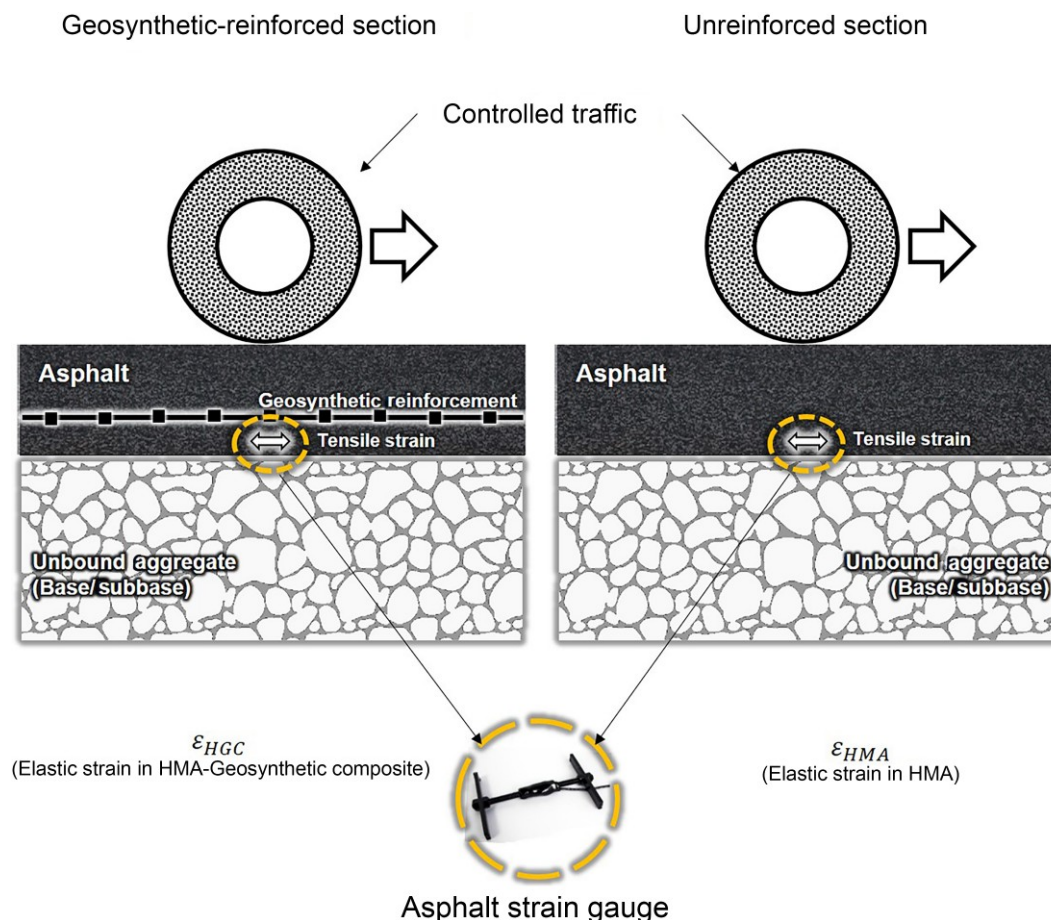


Figure 1. Illustration of full-scale field experiment by Kumar *et al.* (2022, 2025) to measure  $\alpha$

alternatively used to reduce the asphalt thickness. The second approach of the proposed design method involves determining an equivalent axle load factor for HMA-GS Composite ( $EALF_{HGC}$ ), which is subsequently used to determine an equivalent (increased) ESAL, or alternatively used to reduce the design SN, thus, the required thickness for HMA.

It should be noted that the objective of this paper is not to propose a method to obtain or predict  $\alpha$  value for geosynthetic reinforcements, but to propose a design method based on availability of  $\alpha$  to the designer. However, Kumar *et al.* (2022, 2024, 2025) have measured  $\alpha$  for a wide range of geosynthetic reinforcements that can be used as a guide in the absence of other project-specific measurements.

### 2.1. Approach 1: Adopting equivalent modulus of HMA-GS composite ( $E_{HGC}$ )

The proposed design method can be implemented using an approach based on Multi-layer Linear Elastic Analysis (MLEA) to determine an equivalent (increased) modulus for HMA-GS composite. The elastic tensile strain in a geosynthetic-reinforced asphalt road is lower than that in an unreinforced road. Consequently, such reduced elastic tensile strain can be used to back-calculate an equivalent (increased) modulus for HMA-GS Composite ( $E_{HGC}$ ). The procedure involves initially predicting the tensile strain at the bottom of the HMA in an unreinforced road ( $\epsilon_{HMA}$ ) using MLEA. In this case, using design parameters for the unreinforced road including pavement layer thicknesses and material properties (e.g. modulus and Poisson ratio) for asphalt, base and subbase layers, MLEA will estimate  $\epsilon_{HMA}$ . The tensile strain at the bottom of the HMA in the geosynthetic-reinforced asphalt road is then obtained using the tensile strain reduction ratio ( $\alpha$ ), as follows:

$$\epsilon_{HGC} = \alpha \epsilon_{HMA} \quad (2)$$

Finally, MLEA is performed by using the same design parameters as those used for the unreinforced road but by varying the value of the modulus of HMA to back-analyze the equivalent modulus of the HMA-GS Composite (i.e.  $E_{HGC}$ ) that will result in  $\epsilon_{HGC}$  at the bottom of the HMA.

The AASHTO empirical pavement design procedure (AASHTO 1993) established an empirical relationship between a roadway design traffic volume (as quantified by  $ESAL$ ) and the roadway structural capacity (as quantified by  $SN$ ), as follows:

$$\log(ESAL) = \frac{1}{0.40 + \frac{1094}{(SN+1)^{5.19}}} G_t + 9.36 \log(SN+1) - 0.2 + 2.32 \log(M_R) - 8.07 \quad (3)$$

$$G_t = \log\left(\frac{4.2 - p_t}{4.2 - 1.5}\right) \quad (4)$$

where,  $G_t$  is the factor for loss of serviceability,  $p_t$  is the serviceability at the end of time  $t$  and  $M_R$  is the resilient

modulus of the subgrade in psi. For simplicity, Equation (3) does not include the effect of the reliability level. The  $SN$  of an unreinforced road is defined by AASHTO (1993) as:

$$SN = a_1 D_{HMA} + a_2 D_2 m_2 + a_3 D_3 m_3 \quad (5)$$

where,  $D_{HMA}$ ,  $D_2$  and  $D_3$  are the thicknesses of the HMA, base and subbase layers, respectively;  $m_2$  and  $m_3$  are the base and subbase layer drainage coefficients, respectively; and  $a_1$ ,  $a_2$  and  $a_3$  are the HMA, base and subbase layer coefficients, respectively. The layer coefficients have been correlated empirically with the moduli of the corresponding layers, as follows (AASHTO 1993):

$$a_1 = 0.384 (\log E_{HMA}) + 0.184 \quad (6A)$$

$$a_2 = 0.249 (\log E_2) - 0.977 \quad (6B)$$

$$a_3 = 0.227 (\log E_3) - 0.839 \quad (6C)$$

where,  $E_{HMA}$ ,  $E_2$  and  $E_3$  are the moduli of the HMA, base and subbase layers, respectively.

The increased modulus value as determined by MLEA back-analyses (i.e.  $E_{HGC}$ ) for the HMA-GS Composite can be used in Equation (6A) to predict the equivalent (increased) layer coefficient for the HMA-GS Composite layer ( $a'_1$ ) as follows:

$$a'_1 = 0.384 (\log E_{HGC}) + 0.184 \quad (7)$$

The increased modulus of HMA ( $E_{HGC}$ ), as compared to  $E_{HMA}$ , results in a comparatively larger equivalent layer coefficient for HMA ( $a'_1$ ) for the geosynthetic-reinforced asphalt road. The coefficient  $a'_1$  can then be used for the design of the flexible pavement. Two most common design objectives for incorporating geosynthetic reinforcements in flexible pavement involve increasing the traffic volume (for a given HMA layer thickness) or reducing the thickness of the HMA layer (for a given traffic volume).

**Increased Traffic Volume** – If the design objective is to achieve an increased traffic volume (for a given asphalt layer thickness), the increased layer coefficient ( $a'_1$ ) can be used to define an equivalent structural number ( $SN'$ ) for the geosynthetic-reinforced asphalt road with the same HMA thickness as that in the unreinforced road, as follows:

$$SN' = a'_1 D_{HMA} + a_2 D_2 m_2 + a_3 D_3 m_3 \quad (8)$$

The thickness of the geosynthetic-reinforced asphalt layer ( $D_{HMA}$ ) and characteristics of the base and subbase layers (i.e.  $a_2, a_3, D_2, D_3, m_2, m_3$ ) in the reinforced road (Equation (8)) remain the same as those in the unreinforced road (Equation (5)). However, the larger equivalent layer coefficient for HMA ( $a'_1$ ), obtained by adopting  $E_{HGC}$ , results in an increased equivalent structural number ( $SN'$ ) for the geosynthetic-reinforced asphalt road. The increased structural number ( $SN'$ ) is

used in Equation (3) to obtain an increased traffic volume, as follows:

$$\log(ESAL') = \frac{1}{0.40 + \frac{1094}{(SN'+1)^{5.19}}} G_t + 9.36 \log(SN' + 1) - 0.2 + 2.32 \log(M_R) - 8.07 \quad (9)$$

where  $ESAL'$  is the equivalent  $ESAL$  for the geosynthetic-reinforced asphalt road. Comparing Equations (3) and (9), the ratio between the traffic volume in the geosynthetic-reinforced asphalt road and that in the unreinforced road is defined as the Traffic Benefit Ratio with HMA-GS Composite ( $TBR_{HGC}$ ) and determined as follows:

$$TBR_{HGC} = \frac{ESAL'}{ESAL} \quad (10)$$

and

$$\log(TBR_{HGC}) = \left( \frac{1}{0.40 + \frac{1094}{(SN'+1)^{5.19}}} - \frac{1}{0.40 + \frac{1094}{(S+1)^{5.19}}} \right) G_t + 9.36 \log \left( \frac{SN' + 1}{SN + 1} \right) \quad (11)$$

**Reduced HMA Thickness** – Alternatively,  $a'_1$  can be used to achieve the design objective of reducing asphalt thickness (for a given traffic volume). Specifically, for a given  $SN$ , using an equivalent (increased) layer coefficient for the HMA layer facilitates adoption of a reduced HMA thickness and, therefore, the  $SN$  can now be defined as follows:

$$SN = a'_1 D'_{HMA} + a_2 D_2 m_2 + a_3 D_3 m_3 \quad (12)$$

where,  $D'_{HMA}$  is the equivalent (reduced) HMA thickness. The  $SN$  and characteristics of the base and subbase layers (i.e.  $a_2, a_3, D_2, D_3, m_2, m_3$ ) in Equation (12) remain the same as those in the unreinforced road (Equation 5). The  $SN$  of the geosynthetic-reinforced asphalt road (Equation 12) will equal the  $SN$  of the unreinforced road (Equation 5), for the following equivalent HMA layer thickness:

$$D'_{HMA} = \frac{a_1}{a'_1} D_{HMA} \quad (13)$$

Also, the reduction in asphalt thickness ( $\Delta D_{HMA}$ ) is determined as follows:

$$\Delta D_{HMA} = (D_{HMA} - D'_{HMA}) = \left( \frac{a'_1 - a_1}{a'_1} \right) D_{HMA} \quad (14)$$

In summary, designing geosynthetic-reinforced asphalt roads using equivalent modulus of HMA-GS Composite includes the following steps. First, assuming no geosynthetic, design the road for the traffic volume ( $ESAL$ ) and determine the  $SN$  and characteristics of the subbase, base and HMA layers, including the layer coefficient for HMA ( $a_1$ ) and HMA thickness ( $D_{HMA}$ ). Then, use  $\alpha$  with the proposed MLEA procedure to determine the equivalent modulus of HMA-GS Composite ( $E_{HGC}$ ) and use the

obtained  $E_{HGC}$  in Equation (7) to determine the equivalent (increased) layer coefficient for the HMA layer ( $a'_1$ ). If the design objective is to increase the traffic volume, use Equation (8) to determine the equivalent (increased) structural number ( $SN'$ ) for the geosynthetic-reinforced asphalt road, and use  $SN$  and  $SN'$  in Equations (11) and (10) to determine the Traffic Benefit Ratio with HMA-GS Composite ( $TBR_{HGC}$ ) and the equivalent (increased)  $ESAL$  for the geosynthetic-reinforced asphalt road ( $ESAL'$ ). However, if the design objective is to reduce asphalt thickness, use Equation (13) to determine the reduced HMA layer thickness ( $D'_{HMA}$ ), or Equation (14) to determine the asphalt thickness reduction ( $\Delta D_{HMA}$ ).

## 2.2. Approach 2: Adopting equivalent axle load factor for HMA-GS Composite ( $EALF_{HGC}$ )

The second approach to implement the proposed design method involves determining an equivalent axle load factor for HMA-GS composite. The concept of axle load equivalency factor, also known by other terms such as wheel load equivalency or pavement damage factors (Witczak 1981), has been widely used to account for the combined damage of a traffic mix of different axle loads on pavement by converting the pavement damage caused by any axle load to that caused by a standard axle load. Per AASHTO (1993), the equivalent axle load factor ( $EALF$ ) is defined as the ratio between the number of repetitions of an 80-kN (18 kips) standard single axle load and that of a non-standard axle load group to cause the same damage to the road. The  $EALF$  depends on various parameters such as pavement type, thickness, structural capacity, and more importantly the definition of damage. Using the AASHTO empirical equations (Equation (3)) developed after the AASHO Road Test is one of the most widely used methods to determine  $EALF$ . In this case, damage was defined by a certain loss in the serviceability index, determined empirically based on rating the road ride quality by a panel of experts. Accordingly,  $EALF$  for axle load group ' $i$ ' (that is  $EALF_i$ ) is determined as follows:

$$EALF_i = \frac{W_{i18}}{W_{ii}} \quad (15)$$

where  $W_{i18}$  is the total number of standard single axle loads and  $W_{ii}$  is the total number of axle load group ' $i$ ' that cause the same loss of serviceability to a road section.

Alternative mechanistic methods have since been developed to determine  $EALF$  based on critical strains in the pavement (e.g. horizontal tensile strain at the bottom of HMA, vertical compressive strain above the subgrade). In these methods, failure is typically defined either in terms of a certain amount of fatigue cracking or permanent deformations, and  $EALF_i$  is determined as the ratio between the total number of load repetitions to failure, as follows:

$$EALF_i = \frac{N_{f18}}{N_{fi}} \quad (16)$$

where  $N_{f18}$  and  $N_{fi}$  are the number of load repetitions to failure by a load representing the standard single axle load and the axle load group 'i,' respectively. Depending on the test method and definition of failure, the  $EALF$  that is determined by various mechanistic methods may be slightly to largely different from one method to another. A widely accepted mechanistic model has been presented by Asphalt Institute (Asphalt Institute 1982), which was developed based on fatigue cracking in laboratory beam specimens, correlated with field observations. In this case, the failure was defined when a specific percentage of fatigue cracking in the wheel path was observed. The Asphalt Institute model correlates the horizontal tensile strain at the bottom of the HMA layer and the elastic modulus of HMA to the number of load repetition to failure, as follows:

$$N_f = f_1(\varepsilon_i)^{-f_2}(E_{HMA})^{-f_3} \quad (17)$$

where,  $N_f$  is the number of load repetitions to failure;  $\varepsilon_i$  is the elastic tensile strain at the bottom of the HMA layer under the applied load; and the coefficient  $f_1$  and exponents  $f_2$  and  $f_3$  are constants. Other studies have also adopted similar equations but with different values for  $f_1$ ,  $f_2$  and  $f_3$  (e.g. Illinois DOT (Thompson 1987)).

Using Equation (17) into Equation (16),  $EALF_i$  for a certain asphalt mixture can be obtained as follows:

$$EALF_i = \left( \frac{\varepsilon_{ii}}{\varepsilon_{i18}} \right)^{f_2} \quad (18)$$

where  $\varepsilon_{i18}$  and  $\varepsilon_{ii}$  are the elastic tensile strains at the bottom of the HMA layer induced by a load representing the standard single axle and the axle load group 'i,' respectively.

Since the inclusion of geosynthetic reinforcement results in the reduction of tensile strains in the asphalt layer (as quantified by  $\alpha$ ), the damage due to a standard single axle load to the geosynthetic-reinforced asphalt road can be equated to the damage caused by an equivalent (reduced) axle load to the unreinforced road. Therefore, the concept of  $EALF$  was used in this study to predict the reduced effect of a standard single axle load on the HMA-GS Composite. In this case, the  $EALF_{HGC}$  was defined as the ratio between the number of repetitions of a standard single axle load on the unreinforced road ( $W_{i18}$ ) and that on the geosynthetic-reinforced asphalt road ( $W_{i18GS}$ ) to cause the same damage (e.g. same loss in serviceability):

$$EALF_{HGC} = \frac{W_{i18}}{W_{i18GS}} \quad (19)$$

Using the Asphalt Institute mechanistic model, from Equation (18)  $EALF_{HGC}$  can be expressed as follows:

$$EALF_{HGC} = \left( \frac{\varepsilon_{i18GS}}{\varepsilon_{i18}} \right)^{f_2} \quad (20)$$

where,  $\varepsilon_{i18GS}$  and  $\varepsilon_{i18}$  are the elastic tensile strains at the bottom of the HMA under a load representing the

standard single axle load in the geosynthetic-reinforced asphalt and unreinforced roads, respectively.

Using Equation (1),  $\frac{\varepsilon_{i18GS}}{\varepsilon_{i18}}$  in Equation (20) can be replaced by  $\alpha$ , as follows:

$$EALF_{HGC} = (\alpha)^{f_2} \quad (21)$$

Using Equation (19), the total number of standard single axle loads to failure of the geosynthetic-reinforced asphalt road ( $W_{i18GS}$ ) can be expressed as follows:

$$W_{i18GS} = \frac{1}{EALF_{HGC}} W_{i18} \quad (22)$$

Similar to the Equivalent Modulus of HMA-GS Composite approach, formulations were developed here for Equivalent Axle Load Factor for HMA-GS Composite approach for the two design objectives for incorporating geosynthetic reinforcements: increasing the traffic volume (for a given HMA layer thickness) or reducing the thickness of the HMA layer (for a given traffic volume). In the developed formulations,  $EALF_{HGC}$  was used to determine the increased  $ESAL$  for the geosynthetic reinforced asphalt road,  $ESAL'$ , for the objective of increasing the traffic volume. For the objective of reducing HMA thickness,  $EALF_{HGC}$  was used to determine a reduced  $ESAL$  to be used for the design of geosynthetic-reinforced asphalt road,  $ESAL_{Design}$ , which is then used to determine a reduced design  $SN$  and a reduced required HMA thickness. An important aspect in the developed formulations for  $ESAL'$  and  $ESAL_{Design}$  is the reference number of axles used for defining  $ESAL$ . A simplified expression of  $ESAL$  for unreinforced road in terms of  $EALF_i$ ,  $n_i$ , and  $W_{i18}$  is as follows:

$$ESAL = \sum_{i=1}^m EALF_i n_i W_{i18} \quad (23)$$

where  $n_i$  is the percentage of total repetition for the axle load group 'i' and  $m$  is the total number of the axle load groups. In the unreinforced road, damage by any axle load group 'i' is referenced to that caused by a standard single axle load. However, since the damage due to a standard single axle load is different for geosynthetic-reinforced asphalt and unreinforced roads, the reference for determining the  $EALF$  in the two roads may also be considered different. Specifically,  $EALF$  in a geosynthetic-reinforced asphalt road for any axle load group 'i' ( $EALF_{iGS}$ ) may be referenced to the number of repetitions of a standard single axle load on the geosynthetic-reinforced asphalt road ( $W_{i18GS}$ ) (Equation 24A) or to the number of repetitions of a standard single axle load on the unreinforced road ( $W_{i18}$ ) (Equation 24B):

$$EALF_{iGS} = \frac{W_{i18GS}}{W_{iiGS}} \quad (24A)$$

$$EALF_{iGS} = \frac{W_{i18}}{W_{iiGS}} \quad (24B)$$

As further discussed below, Equation (24A) was used in the formulation developed for the design objective of

increasing traffic volume, and Equation (24B) was used in the formulation developed for the design objective of reducing HMA thickness. Furthermore, it was assumed that  $EALF_{iGS}$  from Equation (24A) can be equated to  $EALF$  in the unreinforced road (i.e.  $EALF_i$ ):

$$\frac{W_{t18GS}}{W_{t18}} = \frac{W_{t18}}{W_{t18}} \quad (25)$$

**Increased traffic volume** – For the objective of increasing traffic volume,  $ESAL$  from Equation (23) is expressed with reference to the number of standard single axle loads to failure on the geosynthetic-reinforced asphalt road ( $W_{t18GS}$ ), which is increased compared to that on the unreinforced road:

$$ESAL' = \sum_{i=1}^m EALF_{iGS} n_i W_{t18GS} \quad (26)$$

Accordingly,  $EALF_{iGS}$  is also expressed with reference to  $W_{t18GS}$ , as expressed in Equation (24A).

Using Equations (15) and (25),  $EALF_{iGS}$  in Equation (26) can be replaced by  $EALF_i$ , and using Equation (19),  $W_{t18GS}$  can be replaced by  $W_{t18}/EALF_{HGC}$ :

$$ESAL' = \sum_{i=1}^m EALF_i n_i \frac{W_{t18}}{EALF_{HGC}} \quad (27)$$

Comparing Equations (23) and (27),  $ESAL'$  can be expressed in terms of  $EALF_{HGC}$  and  $ESAL$  as follows:

$$ESAL' = \frac{1}{EALF_{HGC}} ESAL \quad (28)$$

Or the Traffic Benefit Ratio with HMA-GS Composite ( $TBR_{HGC}$ ) can be obtained as follows:

$$TBR_{HGC} = \frac{1}{EALF_{HGC}} \quad (29)$$

**Reduced HMA Thickness** – Alternatively,  $EALF_{HGC}$  can be used to achieve the design objective of reducing asphalt thickness (for a given traffic volume). For this objective,  $ESAL$  from Equation (23) should be expressed with reference to the same number of standard single axle loads as that on the unreinforced road ( $W_{t18}$ ), and accordingly,  $EALF_{iGS}$  should also be expressed with reference to  $W_{t18}$ , as stated in Equation (24B). The equivalent  $ESAL$  in this case is referred to as  $ESAL_{Design}$ , the design (reduced) number of equivalent standard single axle loads adopted for the design of the geosynthetic-reinforced asphalt road:

$$ESAL_{Design} = \sum_{i=1}^m EALF_{iGS} n_i W_{t18} \quad (30)$$

Using Equations (24B), (25), and (19),  $EALF_{iGS}$  in Equation (30) can be replaced by  $EALF_i EALF_{HGC}$ :

$$ESAL_{Design} = \sum_{i=1}^m EALF_i EALF_{HGC} n_i W_{t18} \quad (31)$$

Comparing Equations (23) and (31),  $ESAL_{Design}$  can be expressed in terms of  $EALF_{HGC}$  and  $ESAL$  as follows:

$$ESAL_{Design} = EALF_{HGC} ESAL \quad (32)$$

The AASHTO empirical pavement design equation (AASHTO 1993) for an unreinforced roadway is expressed by Equation (3). The geosynthetic-reinforced asphalt road can be treated as an unreinforced road with equivalent design parameters; thus, Equation (3) was similarly used for the geosynthetic-reinforced asphalt road. Accordingly, the AASHTO flexible pavement design equation was then expressed for the geosynthetic-reinforced asphalt road as follows:

$$\log(ESAL_{Design}) = \frac{1}{0.40 + \frac{1094}{(SN_{Design}+1)^{5.19}}} G_t + 9.36 \log(SN_{Design} + 1) - 0.2 + 2.32 \log(M_R) - 8.07 \quad (33)$$

where,  $SN_{Design}$  is the design (reduced)  $SN$  value when a geosynthetic reinforcement is adopted in the design. Replacing  $\log(ESAL_{Design})$  with  $\log(EALF_{HGC} ESAL)$ , and using Equation (3) to express  $\log(ESAL)$ , Equation (33) was reworked as follows:

$$\log\left(\frac{1}{EALF_{HGC}}\right) = \left(\frac{1}{0.40 + \frac{1094}{(SN+1)^{5.19}}} - \frac{1}{0.40 + \frac{1094}{(SN_{Design}+1)^{5.19}}}\right) G_t + 9.36 \log\left(\frac{SN+1}{SN_{Design}+1}\right) \quad (34)$$

Given the other parameters (i.e.  $SN$ ,  $G_t$  and  $EALF_{HGC}$ ), the above equation can be solved for  $SN_{Design}$ . Considering the definition of structural number,  $SN$  can be expressed as in Equation (5), and  $SN_{Design}$  can be expressed as follows:

$$SN_{Design} = a_1 D'_{HMA} + a_2 D_2 m_2 + a_3 D_3 m_3 \quad (35)$$

Since a smaller design structural number is required for the geosynthetic-reinforced asphalt road to support the same traffic volume as that in the unreinforced road ( $SN_{Design} < SN$ ), a reduced asphalt thickness ( $D'_{HMA}$ ) can be adopted in the design of geosynthetic-reinforced asphalt road. The reduction in asphalt thickness ( $\Delta D_{HMA}$ ) is determined using Equation (5) and (35) as follows:

$$\Delta D_{HMA} = (D_{HMA} - D'_{HMA}) = \frac{SN - SN_{Design}}{a_1} \quad (36)$$

In summary, designing geosynthetic-reinforced asphalt roads using equivalent axle load factor for HMA-GS Composite includes the following steps. First, assuming no geosynthetic, design the road for the design traffic ( $ESAL$ ) and determine the required  $SN$  and characteristics of the subbase, base and HMA layers, including the layer coefficient for HMA ( $a_1$ ) and HMA thickness ( $D_{HMA}$ ). Then, use Equation (21) to obtain  $EALF_{HGC}$ . If the design objective is to increase traffic volume, use  $EALF_{HGC}$  in Equations (28) and (29) to determine the

equivalent (increased) *ESAL* for the geosynthetic-reinforced asphalt road (*ESAL'*) and the Traffic Benefit Ratio with HMA-GS Composite (*TBR<sub>HGC</sub>*). However, if the design objective is to reduce the asphalt thickness, use *SN* and *EALF<sub>HGC</sub>* in Equation (34) to solve for the design (reduced) *SN* when a geosynthetic reinforcement is used (*SN<sub>Design</sub>*). Then, use Equation (36) to determine the reduction in asphalt thickness ( $\Delta D_{HMA}$ ).

### 3. DEVELOPMENT OF DESIGN CHARTS

In this section, the two design approaches that were developed in this study were used along with a typical range of  $\alpha$  to quantify the benefits of adopting geosynthetic reinforcement in the pavement design. Specifically, the suitability of the proposed design approaches is illustrated using design charts that facilitate quantification of the benefits. A design example is also presented in the next section to illustrate the use of design charts. In both the design charts and the design example, it was assumed that the traffic, environmental conditions, and material properties of pavement layers were consistent with those adopted by the Texas Department of Transportation (TxDOT) in the field quantification of  $\alpha$  (Kumar *et al.* 2022, 2024, 2025). Also, similar to the pavement sections by Kumar *et al.* (2022, 2025), the location of the geosynthetic layer was assumed to be in the top half of the asphalt layer. Although the design charts were developed for a specific pavement configuration, the same procedures can be implemented to generate design charts for any other pavement configuration.

#### 3.1. Reference unreinforced road

The unreinforced road considered as the reference for the development of design charts includes subgrade, subbase, base, and HMA layers with the design parameters summarized in Table 1. The values used for the design parameters are within the typical ranges suggested by AASHTO (1993) and TxDOT, and are similar to those used in the design of field sections by Kumar *et al.* (2022, 2025).

The *SN* for the unreinforced road was calculated by determining the structural layer coefficient for each pavement structural layer. The structural layer coefficients for the base ( $a_2$ ) and subbase ( $a_3$ ) were determined using correlations with their modulus values using Equations (6B) and (6C), respectively. The structural layer coefficient for the HMA layer was determined

**Table 1.** Design parameters of pavement layers used to develop design charts

Pavement layer	Thickness (mm)	Modulus (MPa)	Poisson ratio
HMA	$D_{HMA} = 229$	$E_{HMA} = 2,070 \sim 13,800$	0.35
Base	$D_2 = 127$	$E_2 = 345$	0.35
Subbase	$D_3 = 254$	$E_3 = 345$	0.35
Subgrade	Semi-infinite	$M_R = 69$	0.40

using correlations with its modulus. Figure 2 shows the data presented by Van Til *et al.* (1972) to determine the layer coefficient of dense graded HMA using its modulus in semilogarithmic scale. The solid line shows the data presented by Van Til *et al.* (1972) and the dashed line is the regression used in this study. As presented in this figure, a reasonably linear relationship can be interpolated between the modulus of the HMA layer ( $E_{HMA}$ ), in  $10^5$  psi, and its structural layer coefficient ( $a_1$ ) as expressed in Equation (6A).

Using Equation (6A) for the range of HMA modulus values listed in Table 1 results in  $a_1$  ranging from 0.37 (for  $E_{HMA} = 2,070$  MPa) to 0.68 (for  $E_{HMA} = 13,800$  MPa). Accordingly, using Equation (5), the *SN* for this reference unreinforced road ranges from 6.5 (for  $E_{HMA} = 2,070$  MPa) to 9.4 (for  $E_{HMA} = 13,800$  MPa). The drainage coefficients of the base ( $m_1$ ) and subbase ( $m_2$ ) layers were assumed to be equal to 1 in the *SN* calculation, which corresponds to a good quality of drainage for the road where water is removed within a day and the percentage of time pavement structure is exposed to moisture levels approaching saturation is greater than 25% (AASHTO 1993).

#### 3.2. Design of geosynthetic-reinforced asphalt road

In this section, the abovementioned design for the reference unreinforced road was revised considering the inclusion of geosynthetic reinforcement in the HMA layer. While the characteristics of other pavement layers remained the same, the design benefits from incorporating a geosynthetic reinforcement in the asphalt layer were evaluated by a parametric evaluation conducted by varying the design parameters of the HMA layer. The influence of adopting geosynthetic reinforcement in the asphalt layer was introduced by changing  $\alpha$  value. For a wide range of geosynthetic products and pavement conditions, Kumar *et al.* (2022, 2025) found that  $\alpha$  ranged from 1.0 (corresponding to insignificant enhancement by geosynthetic reinforcement) to 0.1 (corresponding to

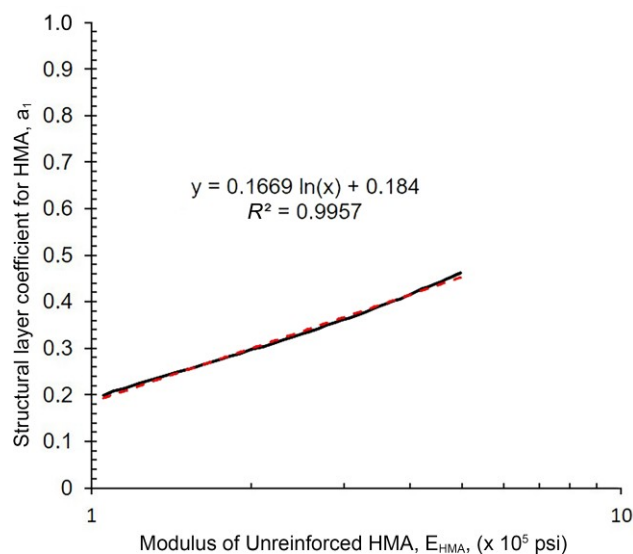


**Figure 2.** Correlation between structural layer coefficient and modulus of HMA (after Van Til *et al.* 1972)

significantly enhanced performance by geosynthetic reinforcement). The design charts presented in this paper were developed for  $\alpha$  value ranging from 0.4 to 0.8.

3.2.1. Design charts for Equivalent Modulus of HMA-GS Composite Approach

3.2.1.1. Equivalent modulus of HMA-GS composite ( $E_{HGC}$ )

Using the Equivalent Modulus of HMA-GS Composite Approach, the increased asphalt modulus for the HMA-GS Composite ( $E_{HGC}$ ) was determined using MLEA. Specifically, the pavement layer properties listed in Table 1 were used in the MLEA to determine the horizontal tensile strain at the bottom of the asphalt layer ( $\epsilon_{HMA}$ ) for different values of  $E_{HMA}$ . Table 2 shows the obtained tensile strains in the second column. Then, the elastic tensile strain at the bottom of the geosynthetic-reinforced HMA ( $\epsilon_{HGC}$ ) was determined using Equation (2) for values of  $\alpha$  ranging from 0.4 to 0.8. Lastly, the same layer properties from Table 1 were used in the MLEA, except that the modulus of the HMA layer was varied to back-analyze the modulus value that results  $\epsilon_{HGC}$ . The obtained modulus values are presented as  $E_{HGC}$  for different values of  $\alpha$  in Table 2.

Figure 3 displays the ratio between  $E_{HGC}$  and  $E_{HMA}$  for different values of  $\alpha$  and  $E_{HMA}$ . As expected, decreasing  $\alpha$  values lead to increasing  $E_{HGC}/E_{HMA}$  ratios, indicating that the equivalent modulus for the HMA-GS

Composite is higher if the geosynthetic reinforcement reduces more significantly the strains in the asphalt layer. As shown by the results presented in this figure, the  $E_{HGC}/E_{HMA}$  ratio was not significantly sensitive to the range of  $E_{HMA}$  (i.e. from 2,070 to 13,800 MPa) used in the analyses, but  $E_{HGC}/E_{HMA}$  had comparatively small variations for different  $E_{HMA}$  values. Accordingly, an average  $E_{HGC}/E_{HMA}$  value was used for the following evaluation purposes in this study, as tabulated in Figure 3. Specifically, the average  $E_{HGC}/E_{HMA}$  ranges from 3.3 (for  $\alpha = 0.4$ ) to 1.3 (for  $\alpha = 0.8$ ), indicating the equivalent modulus of HMA-GS Composite is 1.3 to 3.3 times that of the unreinforced HMA.

3.2.1.2. Equivalent layer coefficient for HMA-GS composite ( $a'_1$ )

The equivalent modulus of the HMA-GS Composite was used in Equation (6A) to determine the equivalent (i.e. increased) structural layer coefficient for HMA-GS Composite ( $a'_1$ ), as follows:

$$a'_1 = 0.384 (\log E_{HGC}) + 0.184 \tag{37}$$

Using the  $E_{HGC}/E_{HMA}$  ratio, Equation (37) is reworked as follows:

$$a'_1 = 0.384 \log \left( \frac{E_{HGC}}{E_{HMA}} E_{HMA} \right) + 0.184 \tag{38}$$

or

Table 2. Results of MLEA for  $\epsilon_{HMA}$  and  $E_{HGC}$

$E_{HMA}$ (MPa)	$\epsilon_{HMA}$	$E_{HGC}$ (MPa) for $\alpha = 0.4$	$E_{HGC}$ (MPa) for $\alpha = 0.5$	$E_{HGC}$ (MPa) for $\alpha = 0.6$	$E_{HGC}$ (MPa) for $\alpha = 0.7$	$E_{HGC}$ (MPa) for $\alpha = 0.8$
2070	5.29E-05	7067	5240	4103	3344	2792
3450	3.61E-05	11 804	8722	6861	5585	4668
6900	2.16E-05	22 698	17 120	13 480	11 101	9274
10 350	1.59E-05	33 193	25 187	20 030	16 720	13 893
13 800	1.28E-05	43 225	32 937	26 298	21 685	18 410

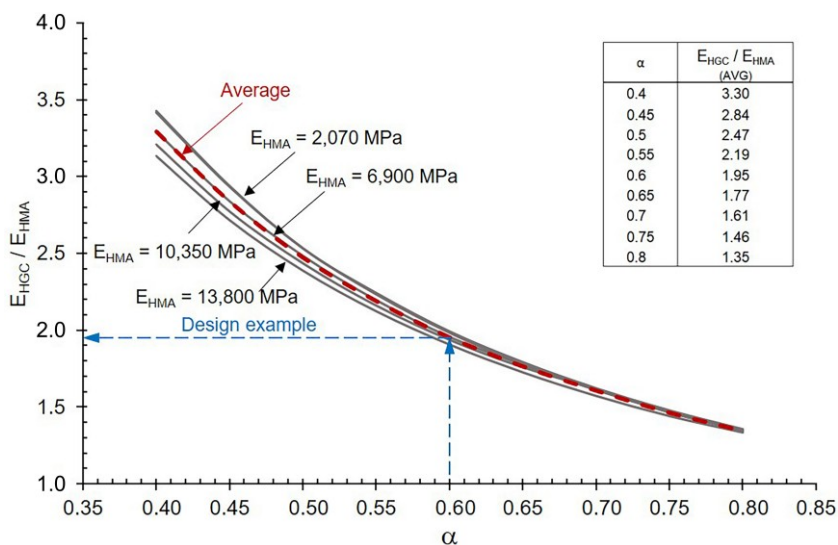


Figure 3. Ratio between equivalent modulus of HMA-GS composite and modulus of unreinforced HMA using MLEA

$$a'_1 = a_1 + 0.384 \log \left( \frac{E_{HGC}}{E_{HMA}} \right) \quad (39)$$

Considering the values obtained for  $E_{HGC}/E_{HMA}$  in Figure 3, the second term in Equation (39) will be a constant for a given  $\alpha$ . Accordingly, design lines to predict  $a'_1$  are parallel to the line for estimating  $a_1$ . The design chart to determine  $a'_1$  for various  $\alpha$  values is presented in Figure 4 along with the original relationship to determine  $a_1$  for the unreinforced road. The input for all design lines (i.e. the horizontal axis in this chart) corresponds to the modulus of the unreinforced HMA ( $E_{HMA}$ ).

**3.2.1.3. Traffic benefit ratio with HMA-GS Composite ( $TBR_{HGC}$ )**

The increased layer coefficient for HMA ( $a'_1$ ) was used in Equation (8) to determine the increased structural

number ( $SN'$ ) for the geosynthetic-reinforced asphalt road. Next,  $SN'$  and  $SN$  were used in Equation (11) to determine the Traffic Benefit Ratio with HMA-GS Composite ( $TBR_{HGC}$ ), the design chart for which can be seen in Figure 5. This figure shows that as the required structural number reduces, geosynthetic reinforcement of HMA can more significantly increase the traffic volume. As  $\alpha$  ranges from 0.8 to 0.4, the traffic benefit ratio ranges from 1.4 to 4 at  $SN = 10$ , and from 1.7 to 7.6 at  $SN = 6$ .

**3.2.1.4. Reduction in HMA layer thickness ( $\Delta D_{HMA}$ )**

Using the corresponding values of  $a'_1$ ,  $a_1$  and  $D_{HMA}$  into Equations (13) and (14), the equivalent (i.e. reduced) HMA thickness for the geosynthetic-reinforced asphalt road ( $D'_{HMA}$ ) and the reduction in the asphalt thickness ( $\Delta D_{HMA}$ ) are determined, respectively. Figure 6 shows the percentage decrease in HMA layer thickness for

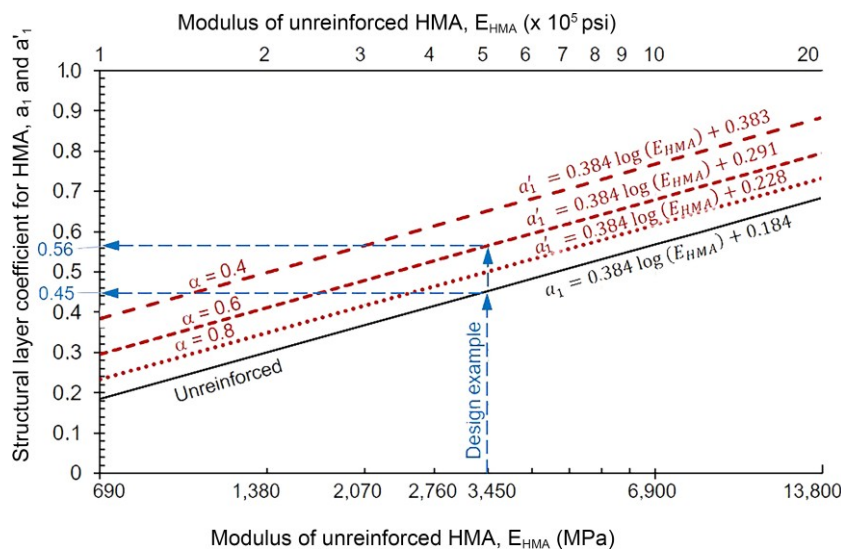


Figure 4. Design chart to predict the equivalent layer coefficient for geosynthetic-reinforced HMA ( $a'_1$ )

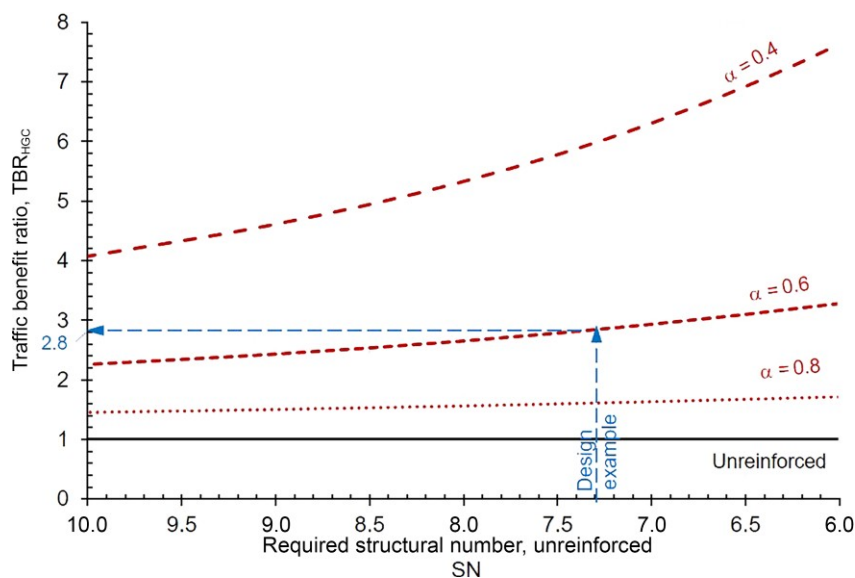
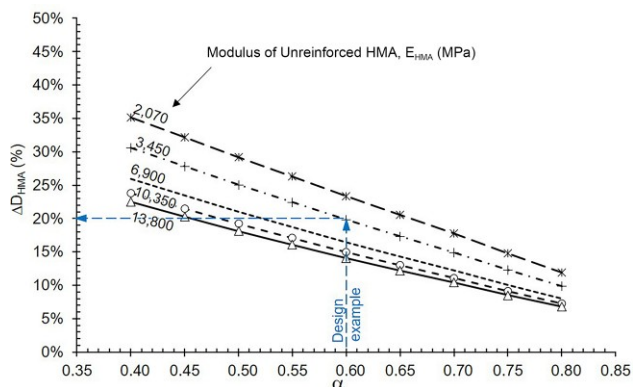


Figure 5. Traffic benefit ratio with HMA-GS composite ( $TBR_{HGC}$ ) in geosynthetic-reinforced asphalt road using equivalent modulus of HMA-GS composite



**Figure 6. Percentage reduction in HMA layer thickness in geosynthetic-reinforced asphalt road using equivalent modulus of HMA-GS composite**

different values of  $\alpha$  and  $E_{HMA}$ . In all cases, the inclusion of a geosynthetic reinforcement significantly reduced the required design thickness of the HMA layer. The percentage reduction in asphalt thickness ranged from approximately 23% to 35% for  $\alpha = 0.4$  and 7% to 12% for  $\alpha = 0.80$ . The benefits from adopting the geosynthetic reinforcement in the asphalt layer were found to diminish for comparatively stiff HMA layers.

**3.2.2. Design charts for equivalent axle load factor for HMA-GS Composite approach**

**3.2.2.1. Equivalent axle load factor for HMA-GS Composite ( $EALF_{HGC}$ ) and traffic benefit ratio with HMA-GS composite ( $TBR_{HGC}$ )**

According to Equation (21),  $EALF_{HGC}$  is a function of  $\alpha$  and  $f_2$ , and according to Equation (29),  $TBR_{HGC}$  is the inverse of  $EALF_{HGC}$ .  $f_2$  is the exponent for strain in transfer functions for fatigue cracking models and varies for different fatigue cracking models. The Asphalt Institute model (Asphalt Institute 1982) and Illinois Department of Transportation (DOT) model (Thompson 1987) are among the most commonly used fatigue cracking models for roadway design. The values adopted for coefficient  $f_1$ , and exponents  $f_2$  and  $f_3$  (Equation (17)) in these models are listed in Table 3.

Using the values in Table 3 for  $f_2$ ,  $EALF_{HGC}$  and thus  $TBR_{HGC}$  can be determined for various  $\alpha$  values. Table 4 presents the obtained values for  $TBR_{HGC}$  for both models along with the average values. Figures 7(a) and 7(b) show  $EALF_{HGC}$  and  $TBR_{HGC}$ , respectively, for different  $\alpha$  values for both models along with the average values. As expected, comparatively greater benefits (i.e. higher traffic benefit ratio) were obtained for low  $\alpha$  values. The traffic volume for the geosynthetic-reinforced asphalt

**Table 3. Constants of fatigue cracking models for Asphalt Institute and Illinois DOT models**

Constant	Asphalt Institute	Illinois DOT
$f_1$	7.96e-2	5e-6
$f_2$	3.291	3
$f_3$	0.854	0

**Table 4. Traffic benefit ratio ( $TBR_{HGC}$ ) using equivalent axle load factor for HMA-GS Composite**

$\alpha$	$TBR_{HGC}$ (Based on Asphalt Institute)	$TBR_{HGC}$ (Based on Illinois DOT)	$TBR_{HGC}$ (Average)
0.4	20.4	15.6	18.0
0.5	9.8	8.0	8.9
0.6	5.4	4.6	5.0
0.7	3.2	2.9	3.1
0.8	2.1	2.0	2.0

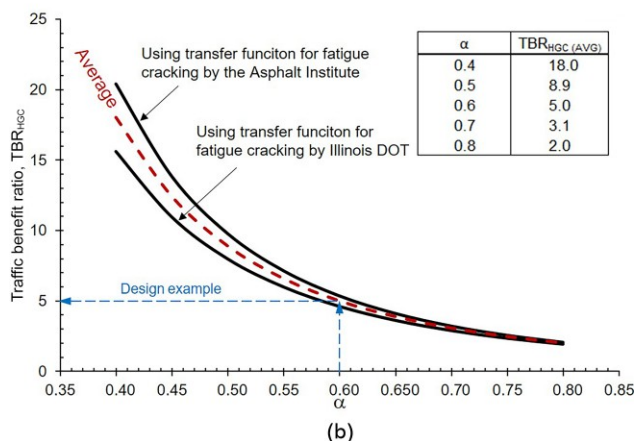
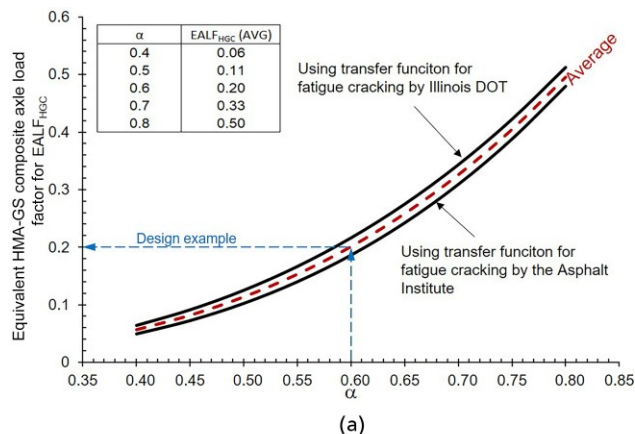


**Figure 7. Design charts based on equivalent axle load factor for HMA-GS composite approach: (a) Equivalent axle load factor for HMA-GS composite ( $EALF_{HGC}$ ); (b) Traffic benefit ratio with HMA-GS composite ( $TBR_{HGC}$ )**

road with  $\alpha = 0.4$  is predicted to be approximately 15 to 20 times that for the unreinforced HMA. At  $\alpha = 0.8$ ,  $TBR_{HGC}$  is similar between the two methods (2.1 using the Asphalt Institute model versus 2.0 using the Illinois DOT model). The average  $TBR_{HGC}$  values in Figure 7(b) indicate that the traffic volume of the geosynthetic-reinforced asphalt road ranges from 2.0 (for  $\alpha = 0.8$ ) to 18 (for  $\alpha = 0.4$ ) times that for the unreinforced road.

**3.2.2.2. Design structural number ( $SN_{Design}$ )**

For the design objective of reducing asphalt thickness, the benefits from adopting geosynthetic reinforcement in the asphalt layer can be expressed by solving Equation (34) to obtain a reduced design structural number ( $SN_{Design}$ ) for the same traffic volume and

serviceability conditions.  $SN_{Design}$  can be obtained for any given  $EALF_{HGC}$ ,  $G_t$  and  $SN$  values. Table 5 summarizes the  $SN_{Design}$  values solved from Equation (34) for  $SN$  values ranging from 1.5 to 10 and  $\alpha$  values of 0.4, 0.6 and 0.8. In this calculation, average  $EALF_{HGC}$  values from Asphalt Institute and Illinois DOT were used. Also, assuming the initial and terminal serviceability as  $p_{t0} = 4.2$  and  $p_{tTerminal} = 2.7$ , respectively, the serviceability loss and factor for terminal loss of serviceability were used as  $\Delta PSI = 1.5$  and  $G_{tTerminal} = -0.26$ , respectively.

Figure 8 shows the relationship between the design  $SN$  for an unreinforced road and a geosynthetic-reinforced asphalt road for different  $\alpha$  values. Each design line in Figure 8 corresponds to a specific value of  $\alpha$ . As expected, the data in Figure 8 confirms that  $SN_{Design}$  decreases as  $\alpha$  decreases, indicating greater benefits from geosynthetic reinforcement.

**3.2.2.3. Equivalent AASHTO 1993 design chart**

An alternative configuration of the design chart for the  $SN$  that is more consistent with the AASHTO 1993 design chart format is presented in Figure 9. This figure shows the AASHTO 1993 design lines to determine the required  $SN$  for unreinforced road along with the design lines proposed in this study for various values of  $\alpha$  to determine the design  $SN$  for geosynthetic-reinforced asphalt road. The input for these design lines (on the vertical axis) is the same as that for the AASHTO 1993 nomographs. However, instead of using the design lines for unreinforced road, the design lines for reinforced

**Table 5. Design  $SN$  for geosynthetic-reinforced asphalt road**

SN (unreinforced road)	SN <sub>design</sub> (reinforced road) for $\alpha = 0.4$	SN <sub>design</sub> (reinforced road) for $\alpha = 0.6$	SN <sub>design</sub> (reinforced road) for $\alpha = 0.8$
10.0	7.0	8.2	9.2
9.0	6.3	7.4	8.3
8.0	5.5	6.5	7.3
7.0	4.7	5.7	6.4
6.0	3.9	4.8	5.4

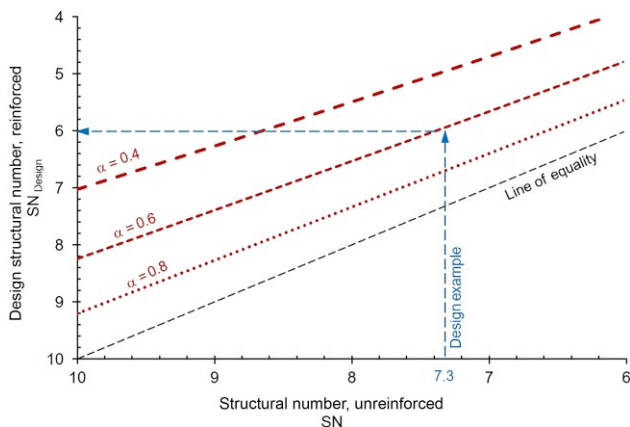


**Figure 8. Design chart to determine design  $SN$  for geosynthetic-reinforced asphalt road based on  $SN$  of an unreinforced road, for same traffic volume**

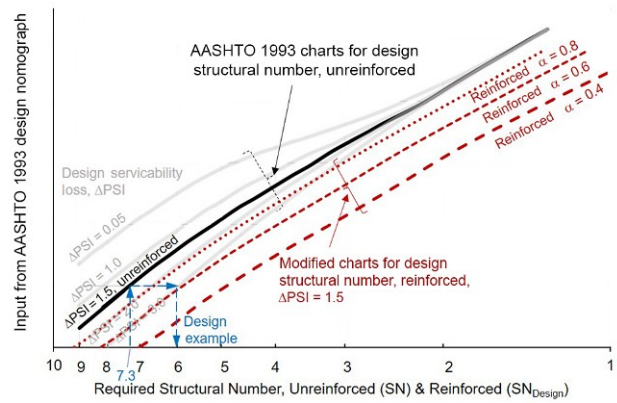


**Figure 9. Modified AASHTO empirical design charts to determine design  $SN$  for geosynthetic-reinforced asphalt road**

road that are developed in this study can be used to determine the design  $SN$ . An example demonstrating the use of this chart is presented in a subsequent section of this paper (see Design Example).

**3.2.2.4. Reduction in HMA layer thickness ( $\Delta D_{HMA}$ )**

The design  $SN$  for the geosynthetic-reinforced asphalt road can be used to reduce the HMA thickness. As expressed in Equation (36), the reduction in HMA thickness ( $\Delta D_{HMA}$ ) can be obtained using  $SN$ ,  $SN_{Design}$  and  $a_1$ . Since the layer coefficient for asphalt ( $a_1$ ) is a function of  $E_{HMA}$ , the absolute asphalt thickness reduction ( $\Delta D_{HMA}$ ) also changes for various  $E_{HMA}$  values. However, the percentage reduction in asphalt thickness will not directly depend on  $E_{HMA}$ , but it depends on  $SN$ ,  $SN_{Design}$ , and characteristics of the base and subbase layers, as follows:

$$\frac{\Delta D_{HMA}}{D_{HMA}} = \frac{\frac{SN - SN_{Design}}{a_1}}{\frac{SN - a_2 D_2 m_2 - a_3 D_3 m_3}{a_1}} = \frac{SN - SN_{Design}}{SN - a_2 D_2 m_2 - a_3 D_3 m_3} \tag{40}$$

Accordingly, using the values obtained above for  $SN$  and  $SN_{Design}$ , and characteristics of the base and subbase layers listed in Table 1,  $\Delta D_{HMA}(\%)$  was calculated as presented in Table 6.

As an alternative presentation of the results in Table 6, Figure 10 presents a collective design chart showing both modification in structural number and reduction in HMA thickness:

1. The design line shown by black solid line on the horizontal axis corresponds to the unreinforced road with  $SN$  ranging from 6 to 10.
2. The red curves correspond to different  $\alpha$  values and show the benefits from adopting geosynthetic reinforcement in the asphalt layer:
  - On the horizontal axis, the range of  $SN$  values corresponding to the red curves indicates that geosynthetic reinforcement could reduce the range of design  $SN$  to 3.9 to 7.0 (for  $\alpha = 0.4$ ), 4.8 to 8.2 (for  $\alpha = 0.6$ ) and 5.4 to 9.2 (for  $\alpha = 0.8$ ).

Table 6. Design SN and percentage reduction in HMA thickness using equivalent axle load factor for HMA-GS composite

$\alpha$	SN = 6 (unreinforced)		SN = 7 (unreinforced)		SN = 8 (unreinforced)		SN = 9 (unreinforced)		SN = 10 (unreinforced)	
	SN <sub>design</sub> (reinforced)	$\Delta D_{HMA}$ (%)	SN <sub>design</sub> (reinforced)	$\Delta D_{HMA}$ (%)	SN <sub>design</sub> (reinforced)	$\Delta D_{HMA}$ (%)	SN <sub>design</sub> (reinforced)	$\Delta D_{HMA}$ (%)	SN <sub>design</sub> (reinforced)	$\Delta D_{HMA}$ (%)
0.4	3.9	77%	4.7	61%	5.5	53%	6.3	47%	7.0	44%
0.6	4.8	45%	5.7	36%	6.5	31%	7.4	28%	8.2	26%
0.8	5.4	20%	6.4	16%	7.3	14%	8.3	13%	9.2	12%

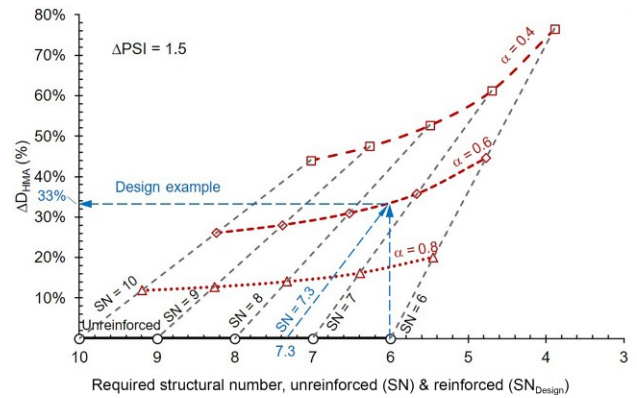


Figure 10. Collective design chart to determine design SN and percentage reduction in HMA thickness using equivalent axle load factor for HMA-GS composite approach

- On the vertical axis, the red curves show the percentage reduction in HMA thickness, indicating that geosynthetic reinforcement could result in a reduction in HMA thickness between 44% and 74% (for  $\alpha = 0.4$ ), between 26% and 45% (for  $\alpha = 0.6$ ) and between 12% and 20% (for  $\alpha = 0.8$ ).
- For a given required SN for unreinforced road, the black dashed curves illustrate the benefits of adopting geosynthetic reinforcement with different  $\alpha$  values. Reductions in the design SN are obtained by projecting these curves on the horizontal axis, and reductions in asphalt thickness are obtained by projecting these curves on the vertical axis.

#### 4. DESIGN EXAMPLE

This section presents a design example to exemplify the use of the proposed modified AASHTO empirical design method for geosynthetic-reinforced asphalt road.

The unreinforced road section adopted in this example is considered to have the base and subbase course characteristics presented in Table 1. Considering a design traffic of 1,020 million *ESAL*, the road design was established to require an SN of 7.3. Considering an HMA layer with a modulus of  $E_{HMA} = 3,450$  MPa (500 ksi) for unreinforced road, the structural layer coefficient for the HMA was obtained as  $a_1 = 0.45$  using the design line presented in Figure 4. Accordingly, the asphalt thickness is determined as  $D_{HMA} = 229$  mm (9 in).

Assume the designer considers using a geosynthetic reinforcement in the middle of the HMA layer that can reduce the elastic tensile strain at the bottom of the HMA by 40% (i.e.  $\alpha = 0.6$ ). Based on the design approaches and design charts presented in this study, alternative designs that can be adopted are as follows:

##### 4.1. Adopting Approach 1

The designer may choose the design approach of using an equivalent modulus for the geosynthetic-reinforced HMA. In this case, an Equivalent Modulus of HMA-

GS Composite ( $E_{HGC}$ ) can be determined using  $\alpha$  and the MLEA procedure elaborated in this study, and accordingly, using Equation (7) the modified layer coefficient for the geosynthetic-reinforced asphalt ( $a'_1$ ) can be obtained. In this example, the design chart in Figure 3 at  $\alpha = 0.6$  can be used to obtain  $E_{HGC}/E_{HMA}$  as 1.95, thus,  $E_{HGC} = 1.95 E_{HMA} = 6,728$  MPa, and the design chart in Figure 4 can be used to obtain  $a'_1$  as 0.56. Then, depending on the design objective, two designs can be developed as follows:

1. To achieve the design objective of increased traffic volume:
  - Using  $a'_1 = 0.56$ , from Equation (8), the equivalent (increased)  $SN$  for the geosynthetic-reinforced asphalt road is obtained as  $SN' = 8.3$ .  $SN$ ,  $SN'$ , and  $G_t$  can then be used in Equation (11) to obtain Traffic Benefit Ratio ( $TBR_{HGC}$ ). Alternatively,  $SN$  can be used in the design chart in Figure 5, to obtain  $TBR_{HGC}$  as 2.8. Thus, the increased traffic volume for the geosynthetic-reinforced asphalt road will be 2.8-fold design  $ESAL$ .
2. To achieve the design objective of reduced asphalt thickness:
  - Using  $a'_1 = 0.56$ ,  $a_1 = 0.45$ , and  $D_{HMA} = 229$  mm in Equation (14), absolute value of reduction in the asphalt thickness can be obtained. Alternatively,  $\alpha = 0.6$  and  $E_{HMA} = 3,450$  MPa can be used in the design chart in Figure 6, to obtain the percentage reduction in HMA thickness as  $\Delta D_{HMA} = 20\%$ ; thus, the HMA thickness for the geosynthetic-reinforced asphalt road is reduced to  $D'_{HMA} = (1 - 0.20)D_{HMA} = 183$  mm.

#### 4.2. Adopting Approach 2

Alternatively, the designer may prefer the design approach of using an equivalent axle load factor for the geosynthetic reinforced HMA. In this case, an Equivalent Axle Load Factor for HMA-GS Composite ( $EALF_{HGC}$ ) can be determined using Equation (21). In this example, the design chart in Figure 7(a) at  $\alpha = 0.6$  and average value of Asphalt Institute and Illinois DOT can be used to obtain  $EALF_{HGC}$  as 0.2. Then, depending on the design objective, two designs can be developed as follows:

1. To achieve the design objective of increased traffic volume:
  - Using Equation (29), the Traffic Benefit Ratio ( $TBR_{HGC}$ ) will be the inverse of  $EALF_{HGC}$ . Alternatively, using  $\alpha = 0.6$  in the design chart in Figure 7(b),  $TBR_{HGC}$  is obtained as 5.0; thus, the increased traffic volume in the geosynthetic-reinforced asphalt road will be 5-fold design  $ESAL$ .
2. To achieve the design objective of reduced asphalt thickness:

- Using  $SN$ ,  $EALF_{HGC}$ , and  $G_t$  in Equation (34), the design (reduced)  $SN$  for the geosynthetic-reinforced asphalt road can be obtained. Alternatively, using  $\alpha = 0.6$  and  $SN = 7.3$  in the design chart in Figure 8,  $SN_{Design}$  is obtained as 6.0. As an additional alternative, the design chart in Figure 9 could be used to obtain  $SN_{Design}$ . In this case, the point corresponding to  $SN = 7.3$  can be projected vertically on the unreinforced roadway design line and then projected horizontally on the design line for  $\alpha = 0.6$  to obtain  $SN_{Design}$  as 6.0 (Figure 9).
- Using  $SN_{Design} = 6.0$ ,  $SN = 7.3$ , and  $a_1 = 0.45$  in Equation (36), the absolute value of reduction in the asphalt thickness can be obtained. Alternatively, from the design chart in Figure 10, either  $SN = 7.3$  or  $SN_{Design} = 6.0$  can be used to determine the percentage reduction in HMA thickness ( $\Delta D_{HMA}(\%)$ ). If  $SN_{Design} = 6.0$  is used on the horizontal axis, the corresponding point on the design chart for  $\alpha = 0.6$  can be obtained by vertical projection. If  $SN = 7.3$  is used, the corresponding point on the design chart for  $\alpha = 0.6$  can be obtained by interpolation between the lines corresponding to  $SN = 7$  and  $SN = 8$ . Using either approach,  $\Delta D_{HMA}(\%)$  is obtained as 33%; thus, the HMA thickness for the geosynthetic-reinforced asphalt road can be reduced to  $D'_{HMA} = (1 - 0.33)D_{HMA} = 153$  mm.

Table 7 summarizes the various alternative designs for the geosynthetic-reinforced asphalt road and compares them with the original design for the unreinforced road. Figure 11 shows a schematic cross-section of the unreinforced road and geosynthetic-reinforced asphalt roads with reduced thicknesses. Since the proposed design approaches follow different design assumptions and concepts, the corresponding design outcomes will not be necessarily the same. Designers may choose to adopt either of the approaches based on consistency of the proposed design assumptions with their envisioned design concept. Selection between the two design benefits (i.e. increased traffic volume vs reduced asphalt thickness) will depend on the project financial strategies and life cycle cost analysis. Achieving increased traffic volume will impose additional initial cost for adopting geosynthetic reinforcement in the asphalt layer while reducing life cycle cost. On the other hand, reducing asphalt thickness may result in the reduced initial capital cost.

## 5. DESIGN IMPLICATIONS

The tensile strain reduction ratios that are referenced in this study were obtained from the full-scale field experiments by Kumar *et al.* (2022, 2025). The field study involved six different geosynthetic products including three polymeric geogrid composites, two fiberglass geogrid composites, and one fiberglass grid. The pre-

**Table 7. Summary of design alternatives in design example**

Design approach	Design parameters	Design assumption	Design benefit due to geosynthetic reinforcement
Unreinforced road AASHTO 1993 Empirical Design	$SN = 7.3$ $E_{HMA} = 3,450 \text{ MPa}$ $a_1 = 0.45$ $D_{HMA} = 229 \text{ mm}$ $ESAL = 1,020 \text{ million}$		
Geosynthetic-reinforced asphalt road ( $\alpha = 0.6$ ) Equivalent Modulus of HMA-GS Composite Design Objective: Increase Traffic Volume	$SN' = 8.3$ $E_{HGC} = 6,728 \text{ MPa}$ $a'_1 = 0.56$ $D_{HMA} = 229 \text{ mm}$ $ESAL' = 2.8 \text{ ESAL}$	Asphalt thickness is the same as that in the unreinforced road	2.8 times the traffic volume of that in the unreinforced road
Design Objective: Reduce Asphalt Thickness	$SN = 7.3$ $E_{HGC} = 6,728 \text{ MPa}$ $a'_1 = 0.56$ $D'_{HMA} = 183 \text{ mm}$ $ESAL = 1,020 \text{ million}$	Traffic volume is the same as that in the unreinforced road	20% reduction in HMA thickness compared to unreinforced road
Equivalent Axle Load Factor for HMA-GS Composite Design Objective: Increase Traffic Volume	$SN = 7.3$ $EALF_{HGC} = 0.2$ $a_1 = 0.45$ $D_{HMA} = 229 \text{ mm}$ $ESAL' = 5 \text{ ESAL}$	Asphalt thickness is the same as that in the unreinforced road	5.0 times traffic volume of that in the unreinforced road
Design Objective: Reduce Asphalt Thickness	$SN_{Design} = 6.0$ $EALF_{HGC} = 0.2$ $a_1 = 0.45$ $D'_{HMA} = 153 \text{ mm}$ $ESAL = 1,020 \text{ million}$	Traffic volume is the same as that in the unreinforced road	33% reduction in HMA thickness compared to unreinforced road

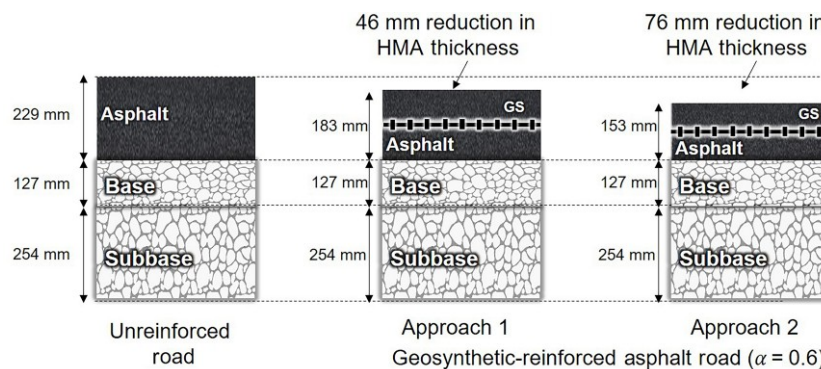


**Figure 11. Schematic profile of an unreinforced roadway and roadways with reduced geosynthetic-reinforced asphalt layer thicknesses: design example**

existing road profile included a 375-mm-thick subbase and base layers overlain by 150-mm-thick asphalt layer, while the rehabilitation comprised repairing the existing asphalt surface, applying binder tack coat, installing geosynthetic interlayer, and finally overlaying with 75-mm-thick asphalt layer. Thus, making a total asphalt layer thickness of 225 mm post rehabilitation (i.e. comprising the pre-existing asphalt and new asphalt overlay). Prior to the roadway rehabilitation, multiple asphalt strain gauges were installed at a depth of 75 mm in the pre-existing asphalt layer (i.e. at a depth of 150 mm from

the final pavement surface) to measure the horizontal tensile strains within the asphalt layer in both longitudinal and transverse directions to traffic.

The location of the field study was in a region that is characterized by a Subtropical Humid climate (Larkin and Bomar 1983). This climate zone is characterized by comparatively short, cold, and wet winters along with warm and long summers. The relative humidity is typically high, and the temperature is rarely below freezing point. Controlled traffic loadings were conducted during September and October months, when the ambient air

temperature ranged between 25°C and 31°C. Although the field study was conducted in the specific climate of east Texas and with project specific road profile and materials, the wide range of geosynthetic products adopted in the study could establish a reasonably acceptable range for  $\alpha$ . It was found that  $\alpha$  ranged from 1.0, the theoretical upper bound of the tensile reduction ratio corresponding to no enhancement by geosynthetic reinforcement, to 0.1, a reasonably small value corresponding to significantly enhanced performance by geosynthetic reinforcement. Potential sources of variability in measurement of  $\alpha$  have been discussed by Kumar *et al.* (2024).

Quantification of project specific  $\alpha$  requires specific information on materials and design parameters including characteristics of geosynthetic reinforcement, subgrade, subbase/base, and asphalt layers, as well as traffic and climatic/environmental conditions. Numerous previous research efforts on the evaluation of performance and quantification of potential benefits from geosynthetic-reinforced asphalt and factors influencing such benefits should also be considered for determining project specific  $\alpha$ . Design benefits predicted in this study shall be further validated by performance evaluations via field, experimental, or numerical research programs until acceptable correlations are established between the predicted benefits and the observed performance.

Overall, although the recent field quantification of  $\alpha$  by Kumar *et al.* (2022, 2024, 2025) has been fundamental in the development of the proposed modified AASHTO design method for geosynthetic-reinforced asphalt road in this study, the proposed design is independent of the method for determining  $\alpha$ . The objective of this paper is not to provide a method to determine  $\alpha$  values for various geosynthetic reinforcements and design conditions, but to propose a design method based on the availability of  $\alpha$  to the designer. Until more extensive research on the most appropriate value of  $\alpha$  for various design conditions becomes available, a project specific value of  $\alpha$  can be determined by using engineering judgement on comparing the specific conditions of the subject design with conditions where  $\alpha$  has been quantified. Prototype field or experimental roadway sections to quantify  $\alpha$  for the specific project conditions would be useful.

## 6. SUMMARY AND CONCLUSIONS

This study presents a modification to the AASHTO 1993 empirical design method for geosynthetic-reinforced asphalt roads. The proposed method relies on the availability of field data to quantify the tensile strain reduction ratio ( $\alpha$ ), which is defined as the ratio between the elastic tensile strain at the bottom of the Hot Mix Asphalt (HMA) layer in a geosynthetic-reinforced asphalt road section and that in a control section (i.e. an equivalent unreinforced road).

The proposed design method can be implemented using an approach in which an equivalent modulus of HMA-GS Composite is determined for the geosynthetic-reinforced HMA which is used to obtain an increased structural layer coefficient for HMA. The increased layer coefficient is then used to determine an equivalent (increased)  $SN$ , and thus, an increased traffic volume, or alternatively a reduced asphalt thickness with the same traffic volume. The second approach defines an Equivalent Axle Load Factor for the HMA-GS Composite (subsequently used to determine an equivalent (increased)  $ESAL$ ), or a reduced design  $SN$  (used to define a reduced required HMA thickness). Specific procedures were developed for each approach to predict the design benefits from adopting geosynthetic reinforcements in the asphalt layer, in terms of an increased traffic volume or a reduced asphalt thickness.

As part of this study, design charts were developed to facilitate the use of the proposed design method with either of the two alternative approaches. While the design charts were developed for pavement configurations typical of those designed by the Texas Department of Transportation (TxDOT), the procedures detailed in this study can be adopted to generate design charts for other pavement configurations as well. Following a comprehensive field evaluation involving roadway sections comprising asphalt layer reinforced with a wide range of geosynthetic reinforcements under various loading conditions, Kumar *et al.* (2022, 2025) determined that  $\alpha$  may generally range from 1.0 (insignificant enhancement by geosynthetic reinforcement) to 0.1 (significantly enhanced performance by geosynthetic reinforcement). The design charts in this paper were developed for  $\alpha$  values ranging from 0.4 to 0.8. Other than conventional parameters used in the design of unreinforced roads,  $\alpha$  is the only additional parameter in the proposed design method that may be determined using experimental or field data along with engineering judgement for project-specific conditions.

Significant design benefits from adopting geosynthetic reinforcement in the asphalt layer were predicted for the specific pavement configurations used in the design charts and design example in this study. The benefits were particularly significant for comparatively lower  $\alpha$  values. Specifically, when adopting the Equivalent Modulus of HMA-GS Composite, it was determined that:

- The average  $E_{HGC}/E_{HMA}$  ranges from 3.30 (for  $\alpha = 0.4$ ) to 1.35 (for  $\alpha = 0.8$ ), indicating that the equivalent modulus of HMA-GS Composite can be expected to be about 1.35 to 3.30-fold that of the unreinforced HMA.
- The traffic benefit ratio of geosynthetic-reinforced asphalt road increases with a decrease in the required structural number for unreinforced road. For  $\alpha$  ranging from 0.8 to 0.4,  $TBR_{HGC}$  ranges from 1.4 to 4 (for  $SN = 10$ ) and from 1.7 to 7.6 (for  $SN = 6$ ).
- The percentage reduction in asphalt thickness is more significant for HMA layers with comparatively low stiffness. As  $\alpha$  ranges from 0.8 to 0.4,  $\Delta D_{HMA}(\%)$

ranges from 12% to 35% for  $E_{HMA} = 2,070$  MPa, and from 7% to 23% for  $E_{HMA} = 13,800$  MPa.

Alternatively, when adopting the Equivalent Axle Load Factor for HMA-GS Composite, it was determined that:

- For  $\alpha$  values ranging from 0.8 to 0.4, the average  $EALF_{HGC}$  was determined to range from 0.5 to 0.06, while the traffic benefit ratio was determined to range from 2 to 18.
- For unreinforced road designs characterized by the required structural number values ranging from 6 to 10, adoption of geosynthetic reinforcement within the asphalt layer can lead to reductions in the required structural number. Specifically, reductions of about 8% to 10% (for  $\alpha = 0.8$ ), about 18% to 20% (for  $\alpha = 0.6$ ), and about 30% to 35% (for  $\alpha = 0.4$ ) were predicted. Higher reductions in required structural number can be achieved for designs involving a larger required structural number.
- The percent reduction in the asphalt thickness due to the inclusion of geosynthetic reinforcement increases when the required structural number for design reduces. As  $\alpha$  ranges from 0.8 to 0.4,  $\Delta D_{HMA}$  (%) is determined to range from 12% to 44% and from 20% to 77% for  $SN = 10$  and 6, respectively.

Overall, the proposed modified AASHTO design method was found to be suitable for the design of roadways with the geosynthetic-reinforced asphalt layer. Further experimental and field calibrations may be needed for full implementation of the proposed design method in various pavement conditions.

## ACKNOWLEDGEMENTS

The authors acknowledge the support received from TxDOT and Huesker, Inc. in the earlier field and experimental research components that led to the development of this design method.

## NOTATION

Basic SI units are given in parentheses.

$a_1$	structural layer coefficient for the unreinforced HMA layer (dimensionless)	$D_3$	thickness of the subbase course (m)
$a'_1$	structural layer coefficient for the geosynthetic-reinforced HMA layer (dimensionless)	$D_{HMA}$	thickness of the unreinforced HMA layer (m)
$a_2$	structural layer coefficient for the base course (dimensionless)	$D'_{HMA}$	thickness of the geosynthetic-reinforced HMA layer (m)
$a_3$	structural layer coefficient for the subbase course (dimensionless)	$E_2$	modulus of the base course (Pa)
$BCR$	base course reduction: percent reduction in base course thickness due to the addition of a geosynthetic (dimensionless)	$E_3$	modulus of the subbase course (Pa)
$D_2$	thickness of the base course (m)	$E_{HMA}$	modulus of the unreinforced HMA layer (Pa)
		$E_{HGC}$	equivalent (increased) modulus of HMA-GS Composite (Pa)
		$EALF$	Equivalent Axle Load Factor: ratio between the number of repetitions of a standard single axle load and that of a non-standard axle load group to cause the same damage to the road (dimensionless)
		$EALF_{HGC}$	Equivalent Axle Load Factor for HMA-GS Composite: ratio between the number of repetitions of a standard single axle load on an unreinforced road and that on the geosynthetic-reinforced asphalt road to cause the same damage (dimensionless)
		$EALF_i$	ratio between the number of repetitions of a standard single axle load and that of a non-standard axle load group ' $i$ ' to cause the same damage to an unreinforced road (dimensionless)
		$EALF_{iGS}$	ratio between the number of repetitions of a standard single axle load in an unreinforced road or in geosynthetic-reinforced asphalt road and that of a non-standard axle load group ' $i$ ' to cause the same damage to the geosynthetic-reinforced asphalt road (dimensionless)
		$ESAL$	Equivalent Single Axle Load for the unreinforced road: number of 80 kN (18-kip) equivalent single axle load applications for a pavement structure over the selected design life (dimensionless)
		$ESAL'$	equivalent (increased) $ESAL$ for the geosynthetic-reinforced asphalt road (dimensionless)
		$ESAL_{Design}$	design (reduced) $ESAL$ adopted for design of geosynthetic-reinforced asphalt road (dimensionless)
		$f_1$	coefficient in the transfer function for fatigue cracking models (dimensionless)
		$f_2$	exponent in the transfer function for fatigue cracking models (dimensionless)
		$f_3$	exponent in the transfer function for fatigue cracking models (dimensionless)
		$G_t$	factor for loss of serviceability (dimensionless)
		$G_{tTerminal}$	factor for terminal loss of serviceability (dimensionless)
		$m$	total number of axle load groups in defining $ESAL$ (dimensionless)
		$m_2$	drainage coefficient for the base course (dimensionless)
		$m_3$	drainage coefficient for the subbase course (dimensionless)

$M_R$	resilient modulus of the subgrade (Pa)	$\varepsilon_{HGC}$	elastic tensile strain at the bottom of the HMA layer in geosynthetic-reinforced asphalt road (dimensionless)
$N_f$	number of load repetitions to failure in fatigue cracking models (dimensionless)	$\varepsilon_{ti}$	elastic tensile strains at the bottom of the HMA layer in an unreinforced road induced by a load representing the axle load group 'i' (dimensionless)
$N_{fi}$	number of load repetitions to failure by a load representing axle load group 'i' (dimensionless)	$\varepsilon_t$	elastic tensile strain at the bottom of the HMA layer in fatigue cracking models (dimensionless)
$N_{f18}$	number of load repetitions to failure by a load representing the standard single axle load (dimensionless)	$\varepsilon_{t18}$	elastic tensile strain at the bottom of the HMA layer in an unreinforced road induced by a load representing the standard single axle load (dimensionless)
$n_i$	percentage of total repetition for the axle load group 'i' in defining <i>ESAL</i> (dimensionless)	$\varepsilon_{t18GS}$	elastic tensile strain at the bottom of the HMA layer in geosynthetic-reinforced road induced by a load representing the standard single axle load (dimensionless)
$p_t$	serviceability at time <i>t</i> (dimensionless)		
$p_{t0}$	initial serviceability index (dimensionless)		
$P_{tTerminal}$	terminal serviceability index (dimensionless)		
$SN$	structural number for an unreinforced road (dimensionless)		
$SN'$	equivalent (increased) <i>SN</i> for the geosynthetic-reinforced asphalt road (dimensionless)		
$SN_{Design}$	design (reduced) <i>SN</i> adopted for design of geosynthetic-reinforced asphalt road (dimensionless)		
$TBR$	Traffic Benefit Ratio: ratio between the traffic volume on a geosynthetic-reinforced roadway and that on an equivalent unreinforced roadway for a prescribed rut depth (dimensionless)		
$TBR_{HGC}$	Traffic Benefit Ratio with HMA-GS Composite: ratio between the traffic volume on the geosynthetic-reinforced asphalt road and that on an unreinforced road (dimensionless)		
$W_{t18}$	total number of standard single axle loads that cause terminal loss of serviceability to an unreinforced road (dimensionless)		
$W_{t18GS}$	total number of standard single axle loads that cause terminal loss of serviceability to geosynthetic-reinforced asphalt road (dimensionless)		
$W_{ti}$	total number of axle load group 'i' that cause terminal loss of serviceability to an unreinforced road (dimensionless)		
$W_{tiGS}$	total number of axle load group 'i' that cause terminal loss of serviceability to geosynthetic-reinforced asphalt road (dimensionless)		
$\alpha$	tensile strain reduction ratio: ratio between the elastic tensile strain at the bottom of the HMA layer in a geosynthetic-reinforced asphalt road and that in an equivalent unreinforced road (dimensionless)		
$\Delta D_{HMA}$	reduction in HMA thickness due to the inclusion of geosynthetic reinforcement in the asphalt layer (m)		
$\Delta PSI$	serviceability loss (dimensionless)		
$\varepsilon_{HMA}$	elastic tensile strain at the bottom of the HMA layer in an unreinforced road (dimensionless)		

## ABBREVIATIONS

AASHO	American Association of State Highway Officials
AASHTO	American Association of State Highway and Transportation Officials
ASG	asphalt strain gauge
GS	geosynthetic
HGC	HMA-GS composite
HMA	hot mix asphalt
MLEA	multi-layer linear elastic analysis
TxDOT	Texas department of transportation

## REFERENCES

- AASHTO (1993). *Guide for Design of Pavement Structures*. American Association of State Highway and Transportation Officials, Washington, DC, USA.
- AASHTO (2009). *Geosynthetic Reinforcement of the Aggregate Base Course of Flexible Pavement Structures. Standard Practice R50-09*, American Association of State Highway and Transportation Officials, Washington, DC, USA.
- Al-Qadi, I. L., Tutumluer, E. & Dessouky, S. (2006). Construction and instrumentation of full-scale geogrid-reinforced flexible pavement test sections. In *Proceedings of the Highway Pavements & Airfield Technology Conference, Atlanta, GA, USA*, Al-Qadi, I. L., Editor, ASCE, Reston, VA, USA, pp. 131–142.
- Asphalt Institute (1982). *Research and Development of the Asphalt Institute's Thickness Design Manual (MS-1)*. 9th edn. Research Report No. 82-2, August 1982.
- Berg, R. R., Christopher, B. R. & Perkins, S. W. (2000). *Geosynthetic reinforcement of the aggregate base/subbase courses of flexible pavement structures-GMA white paper II*. Geosynthetic Materials Association, Roseville, MN, USA, 176.
- Brown, S. F., Thom, N. H., Sanders, P. J., Brodrick, B. V. & Cooper, S. (1999). *Reinforced asphalt, Final report to Tensar International, ABG Ltd, Maccaferri Ltd., Scott Wilson Pavement Engineering, Bardonia Aggregates, and 6D Solutions*. Report No. PGR 99025. University of Nottingham, School of Civil Engineering, UK.
- Brown, S. F., Thom, N. H. & Sanders, P. J. (2001). A study of grid reinforced asphalt to combat reflection cracking. *Journal of Association of Asphalt Paving Technologists*, **70**, 543–571.
- Correia, N. S. & Zornberg, J. G. (2016). Mechanical response of flexible pavements enhanced with geogrid-reinforced asphalt overlays. *Geosynthetics International*, **23**, No. 3, 183–193.

- Cuelho, E., Perkins, S. & Morris, Z. (2014). *Relative Operational Performance of Geosynthetics Used as Subgrade Stabilization*, Report FHWA/MT-14-002/7712-251. Western Transportation Institute, Montana State University – Bozeman, Bozeman, MT, USA.
- Elseifi, M. A. (2003). *Performance Quantification of Interlayer Systems in Flexible Pavements Using Finite Element Analysis, Instrument Response and Non-Destructive Testing*. PhD Thesis, Virginia Polytechnic Institute and State University, Virginia, USA.
- Ferrotti, G., Canestrari, F., Pasquini, E. & Virgili, A. (2012). Experimental evaluation of the influence of surface coating on fiberglass geogrid performance in asphalt pavements. *Geotextiles and Geomembranes*, **34**, 11–18.
- Freire, R., Di Benedetto, H., Sauzeat, C., Pouget, S. & Lesueur, D. (2023). Rational design method for bituminous pavements reinforced by geogrid. *Geotextiles and Geomembranes*, **51**, No. 5, 39–52.
- Graziani, A., Pasquini, E., Ferrotti, G., Virgili, A. & Canestrari, F. (2014). Structural response of grid-reinforced bituminous pavements. *Materials and Structures*, **47**, No. 8, 1391–1408.
- Giroud, J. P. & Noiray, L. (1981). Geotextile-reinforced un-paved road design. *Journal of Geotechnical Engineering Division*, **107**, No. GT9, 1233–1254.
- Giroud, J. P. & Han, J. (2004). Design method for geogrid-reinforced unpaved roads: I. development of design method. *Journal of Geotechnical and Geoenvironmental Engineering*, **130**, No. 8, 775–786.
- Kumar, V. V., Saride, S. & Zornberg, J. G. (2021a). Mechanical response of full-scale geosynthetic-reinforced asphalt overlays subjected to repeated loads. *Transportation Geotechnics*, **30**, 100617, [10.1016/j.trgeo.2021.100617](https://doi.org/10.1016/j.trgeo.2021.100617).
- Kumar, V. V., Saride, S. & Zornberg, J. G. (2021b). Fatigue performance of geosynthetic-reinforced asphalt layers. *Geosynthetics International*, **28**, No. 6, 584–597.
- Kumar, V. V., Roodi, G. H., Subramanian, S. & Zornberg, J. G. (2022). Influence of asphalt thickness on performance of geosynthetic-reinforced asphalt: full-scale field study. *Geotextiles and Geomembranes*, **50**, No. 5, 1052–1059.
- Kumar, V. V., Roodi, G. H., Subramanian, S., Saxena, A., Blake, C. & Zornberg, J. G. (2024). *Geosynthetic Reinforcement in Asphalt Overlays for Increased Roadway Structural Capacity*. Rep. No. FHWA/TX-25/0-7002-1, Texas DOT, Austin, TX, USA.
- Kumar, V. V., Roodi, G. H. & Zornberg, J. G. (2025). Influence of paving interlayer material on performance of full-scale asphalt overlays. In *Proceedings of Geotechnical Frontiers, GSP 364*, pp. 454–463.
- Kunst, P. A. J. E. & Kirschner, R. (1993). Investigation on the effectiveness of synthetic asphalt reinforcements. In *Proceedings of the 2<sup>nd</sup> International Conference on Reflective Cracking in Pavements*, Liege, pp. 187–192.
- Larkin, T. J. & Bomar, G. W. (1983). *Climatic Atlas of Texas*. Texas Department of Water Resources. Texas Department of Water Resources, Austin, TX, USA, pp. LP–192.
- Lytton, R. L. (1989). Use of geotextiles for reinforcement and strain relief in asphalt concrete. *Geotextiles and Geomembranes*, **8**, No. 3, 217–237.
- Molenaar, A. A. A. (1995). *Design method for plain and Hatelit reinforced overlays on cracked pavements*. Delft University of Technology, Delft, Netherlands.
- Molenaar, A. A. A. & Nods, M. (1996). Design method for plain and geogrid reinforced overlays on cracked pavements. In *Proceedings of the 3rd International RILEM Conference on Reflective Cracking in Pavements*, Maastricht, Netherlands, pp. 311–320.
- Pasquini, E., Bocci, M. & Canestrari, F. (2014). Laboratory characterization of optimized geocomposites for asphalt pavement reinforcement. *Geosynthetic International*, **21**, No. 1, 24–36.
- Perkins, S. W., Christopher, B. R., Cuelho, E. L., Eiksund, G. R., Hoff, I., Schwartz, C. W., Svanø, G. & Want, A. (2004). *Development of Design Methods for Geosynthetic Reinforced Flexible Pavements*. US DOT, Federal Highway Administration, Washington, DC, USA.
- Roodi, G. H., Zornberg, J. G., Yang, L. & Kumar, V. V. (2023). Cross-Shear test for geosynthetic-reinforced asphalt. *Transportation Geotechnics*, **38**, 100902.
- SABITA TG3 (2022). *Technical Guideline: Asphalt reinforcement for road construction*. 3rd edn. South African Bitumen Association, Howard Place, South Africa.
- Saride, S. & Kumar, V. V. (2017). Influence of geosynthetic-interlayers on the performance of asphalt overlays on pre-cracked pavements. *Geotextiles and Geomembranes*, **45**, No. 3, 184–196.
- Solatiyan, E., Bueche, N. & Carter, A. (2020). A review on mechanical behavior and design considerations for reinforced-rehabilitated bituminous pavements. *Construction and Building Materials*, **257**, 119483, [10.1016/j.conbuildmat.2020.119483](https://doi.org/10.1016/j.conbuildmat.2020.119483).
- Sprague, C. J. & Sprague, J. E. (2016). Full-scale trafficking of geosynthetic-reinforced road sections. In *Proceedings of 3rd Pan-American Conference on Geosynthetics*, Miami Beach, FL, USA. Industrial Fabrics Association International (IFAI), St Paul, MN, USA, pp. 1992–2001.
- Stewart, J., Williamson, R. & Mohny, J. (1977). *Guidelines for Use of Fabrics in Construction and Maintenance of Low-Volume Roads*. Federal Highway Administration, Washington, DC, USA.
- Tang, X., Abu-Farsakh, M., Hanandeh, S. & Chen, Q. (2014). Use of geosynthetics for reinforcing/stabilizing unpaved roads under full-scale truck axle loads. In *Proceedings of the Shale Energy Engineering Conference*, Pittsburgh, PA, USA, Meehan C. L., VanBriesen J. M., Vahedifard F., Yu X. and Quiroga C., Editors, ASCE, Reston, VA, USA, pp. 591–602.
- Thompson, M. R. (1987). ILLI-PAVE Based Full-Depth Asphalt Concrete Pavement Design Procedure. In *Proceedings of the 6<sup>th</sup> International Conference on Structural Design of Asphalt Pavements*, Vol. 1, pp. 13–22.
- Van Til, C. J., McCullough, B. F., Vallergera, B. A. & Hicks, R. G. (1972). *Evaluation of AASHO Interim Guides for Design of Pavement Structures*. NCHRP Report 128, Highway Research Board, Washington, DC, USA, p. 124.
- Witczak, M. W. (1981). *Equivalent Wheel Load Factors*. Report prepared for Association of American Railroads. University of Maryland, Feb. 1981.
- Zofka, A. & Maliszewski, M. (2019). Practical overlay design for geogrid reinforcement of asphalt layers. *Road Materials and Pavement Design*, **20**, No. Sup1, S163–S182.
- Zornberg, J. G. (2017). Functions and applications of geosynthetics in roadways. *Procedia Engineering*, **189**, 298–306.

The Editor welcomes discussion on all papers published in *Geosynthetics International*. Please email your contribution to [discussion@geosynthetics-international.com](mailto:discussion@geosynthetics-international.com) by 15 October 2026